Hindawi Publishing Corporation
International Journal of Antennas and Propagation
Volume 2016, Article ID 2623617, 11 pages
http://dx.doi.org/10.1155/2016/2623617

Research Article

Cognitive MIMO Frequency Diverse Array Radar with High LPI Performance

Ling Huang,[1,2] Kuandong Gao,[1] Zhiming He,[1] and Jingye Cai[1]

[1]*College of Electronic Engineering and School of Communication and Information Engineering, University of Electronic Science and Technology of China, Chengdu 611731, China*
[2]*School of Electronic and Information Engineering, Lanzhou University of Technology, Lanzhou 737500, China*

Correspondence should be addressed to Kuandong Gao; kuandonggao@gmail.com

Received 1 January 2016; Revised 7 April 2016; Accepted 3 May 2016

Academic Editor: Aboulnasr Hassanien

Frequency diverse array (FDA) has its unique advantage in realizing low probability of intercept (LPI) technology for its dependent beam pattern. In this paper, we proposed a cognitive radar based on the frequency diverse array multiple-input multiple-output (MIMO). To implement LPI of FDA MIMO transmit signals, a scheme for array weighting design is proposed, which is to minimize the energy of the target location and maximize the energy of the receiver. This is based on the range dependent characteristics of the frequency diverse array transmit beam pattern. To realize the objective problem, the algorithm is proposed as follows: the second-order nonconvex optimization problem is converted into a convex problem and solved by the bisection method and convex optimization. To get the information of target, the FDA MIMO radar is proposed to estimate the target parameters. Simulation results show that the proposed approach is effective in decreasing the detection probability of radar with lossless detection performance of the receive signal.

1. Introduction

In the modern battlefield, active surveillance radars are highly vulnerable to detection and exploitation by opposing forces. The ongoing battle between radar systems and the electronic devices used to exploit, degrade, or prevent radar operation has been termed electronic warfare (EW) [1]. In light of the significant threat presented by electronic support measures receivers, there has been a growing trend towards the development of low probability of intercept (LPI) radar systems. Numerous techniques have been proposed to lower the detection probability by the electronic support measures receivers of targets [2–4]. These technologies include high duty cycle, wideband waveforms, lower sidelobes, and broader antenna beam pattern [5, 6]. However, these methods can not decrease the detection probability of the radar transmit signal by the target and increase the detection probability of reflected signal by radar receiver. In this paper, we propose an FDA MIMO cognitive radar to implement LPI by the electronic support measures receivers.

Different from phased array, a small frequency increment, as compared to the carrier frequency, is applied between the FDA elements [7–11]. This small frequency increment results in a range-angle-dependent beam pattern [12–14]. The time and angle periodicity of FDA beam pattern was analyzed in [15]. A linear FDA was proposed in [16] for forward-looking radar ground moving target indication. The application of FDA to bistatic system was analyzed in [17]. And the imaging of FDA radar is investigated in [18–20]. In [21], we have investigated the FDA Cramér-Rao lower bounds (CRLB) for estimating direction, range, and velocity. Although recently FDA has drawn much attention in antenna and radar areas, existing literatures mainly concentrate on FDA conceptual system design [22, 23]. Furthermore, for FDA MIMO radar system, most of the literatures investigated its beamforming technology [24–26], and little work focused on its signal detection applications [27, 28].

In this paper, we propose a cognitive FDA MIMO radar to realize LPI. The cognitive FDA MIMO radar includes two sections. (1) For receive array, FDA MIMO radar is used to

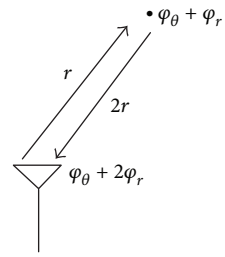

Figure 1: The different phases of radar signal caused by range.

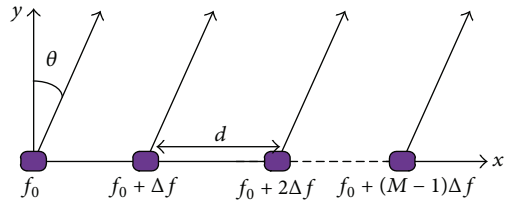

Figure 2: The FDA structure.

detect the reflected signals and estimate the target parameters. (2) For transmit array, the weighting vector design is used to get LPI radar signals. The LPI principle of FDA MIMO radar is introduced as follows: as shown in Figure 1, the transmit signal by one element of antenna makes the target arrive at the range r; the signal phases caused by angle and range are φ_θ and φ_r, respectively. When the signal is reflected by the target and received by MIMO radar, φ_θ is not changed and the phase caused by range becomes $2\varphi_r$. So the signal phases are different at the target and the receiver. Based on these, we employ the range dependent beam pattern of FDA MIMO radar to implement LPI for active radar in this paper. To lower the detection probability of FDA MIMO radar transmit signal, we design the transmit beam pattern with low power at the target location which is difficult to detect by electronic support measures receivers. After being reflected by the target, the designed signal beam pattern has higher power and the receiver detected it easily.

The rest of this paper is organized as follows. In Section 2, we formulate the FDA radar data model. And we present a cognitive radar with FDA MIMO location and FDA MIMO transmit beam pattern design in Section 3. Simulation results are provided in Section 4. Finally, conclusions are drawn in Section 5.

2. Data Model of FDA Radar

Suppose an M-element uniform linear FDA with interelement spacing denoted as d, as shown in Figure 2. The radiated frequency from the mth element is as follows:

$$f_m = f_0 + m\Delta f, \quad m = 0, 1, 2, \ldots, M-1, \tag{1}$$

where f_0 and Δf are the carrier frequency and frequency increment, respectively. Taking the first element as the reference for the array, under far-field condition, one might express the direct wave component of the electric field emitted from the FDA at the observation point (θ, r) as [26]

$$A(\theta, r, t) = \sum_{m=0}^{M-1} a_m \varsigma_m(\theta \mid w_m) \frac{e^{jw_m(t-(r+d_m \sin\theta)/c_0)}}{r}, \tag{2}$$

where M is the number of FDA elements, a_m represents the complex excitation coefficient for the mth element, $\varsigma_m(\theta \mid w_m)$ stands for the far-field vector radiation pattern for the mth element at range r and angular frequency $w_m = 2\pi f_m$, c_0 is the light speed, d_m is the element position of the mth element reference relative to the first element, and t is the time parameter. In accordance with the far-field assumption, $e^{jw_m(t-(r+d_m \sin\theta)/c_0)}/r$ corresponds to the delayed carrier with free space loss.

To interpret the effect of frequency diversity within the scope of an array factor, we should factor the vector element pattern out of (2). This can indeed be done under certain conditions. Assuming all elements in the FDA are identical, we can eliminate the frequency dependence in the element factor; we have

$$\varsigma_m(\theta \mid w_m) \approx \varsigma(\theta \mid w_0), \tag{3}$$

where w_0 is the carrier angular frequency. So (2) can be rewritten as

$$A(\theta, r, t) = \varsigma(\theta \mid w_0) \sum_{m=0}^{M-1} a_m \frac{e^{jw_m(t-((r+d_m \sin\theta)/c_0))}}{r}. \tag{4}$$

Further simplification becomes possible by considering particular FDA arrangements that are simple to handle and yet able to provide valuable insight. By definition, the elements are excited with uniform amplitude; there is a phase progression across the adjacent array elements. These

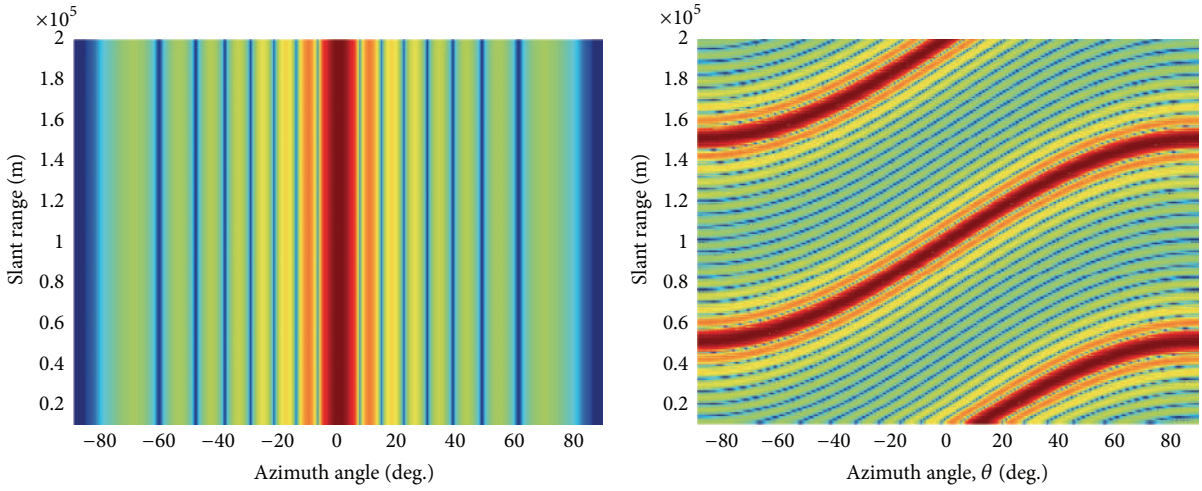

FIGURE 3: Comparative beam pattern between conventional phased array and FDA, where $t = 0$, $\Delta f = 3\,\text{kHz}$, $M = 8$, $f_0 = 10\,\text{GHz}$, and $d = \lambda/2$ with λ being the wavelength assumed. (a) Phased-array radar; (b) FDA radar.

specifications translate to the following expressions for d_m and a_m:

$$\begin{aligned} d_m &= md, \\ a_m &= e^{-jm\phi_a}, \end{aligned} \tag{5}$$

where ϕ_a stands for the phase progression. Submitting (1) and (5) into (4) yields

$$\begin{aligned} A(\theta, r, t) &= \varsigma(\theta \mid w_0) \\ &\cdot \sum_{m=0}^{M-1} e^{-jm\phi_a} \frac{e^{j2\pi(f_0+m\Delta f)(t-((r+md\sin\theta)/c_0))}}{r} = \frac{\varsigma(\theta \mid w_0)}{r} \\ &\cdot e^{j\varphi_0} \sum_{m=0}^{N-1} e^{-jm\phi_a} e^{j2\pi m\Delta f(t-((r+md\sin\theta)/c_0))-j2\pi f_0(md\sin\theta/c_0)}, \end{aligned} \tag{6}$$

where $\varphi_0 = 2\pi f_0 t - 2\pi f_0(r/c_0)$. For notation convenience, we define $\bar{\varsigma} = \varsigma(\theta \mid w_0)e^{j2\pi f_0 t - j2\pi f_0(r/c_0)}$. Equation (6) can then be rewritten as

$$\begin{aligned} &A(\theta, r, t) \\ &= \frac{\bar{\varsigma}}{r} \sum_{m=0}^{M-1} e^{-jm\phi_a} e^{j2\pi m(t\Delta f-((r+md\sin\theta)/c_0)\Delta f - f_0(d\sin\theta/c_0))}. \end{aligned} \tag{7}$$

Since $md\sin\theta \ll r$ and Δf is a very small frequency increment, (7) can be reformulated as

$$\begin{aligned} A(\theta, r, t) &\approx \frac{\bar{\varsigma}}{r} \sum_{m=0}^{M-1} e^{-jm\phi_a} e^{j2\pi m(t\Delta f-(r/c_0)\Delta f - f_0(d\sin\theta/c_0))} \\ &= \frac{\bar{\varsigma}}{r} \mathbf{w}^H \mathbf{v}(\theta, r, t), \end{aligned} \tag{8}$$

where

$$\begin{aligned} \mathbf{w} &= \left[1 \;\; e^{j\phi_a} \;\; \cdots \;\; e^{j(M-1)\phi_a}\right]^T, \\ \mathbf{v}(\theta, r, t) &= \left[1 \;\; e^{j2\pi(t\Delta f-(r/c_0)\Delta f - f_0(d\sin\theta/c_0))} \;\; \cdots \;\; e^{j2\pi(M-1)(t\Delta f-(r/c_0)\Delta f - f_0(d\sin\theta/c_0))}\right]^T, \end{aligned} \tag{9}$$

with $[\cdot]^T$ and $[\cdot]^H$ being the transpose operator and Hermitian transpose operator, respectively. For simplicity, $\bar{\varsigma} = 1$ is assumed in the following discussions. Figure 3 shows the beam pattern of phased-array beam pattern and FDA beam pattern. We can see that the FDA beam pattern is dependent on range and angle. However, the phased-array beam pattern is only dependent on the angle. The range dependent FDA beam pattern provides the LPI capability for FDA MIMO cognitive radar.

3. Cognitive FDA MIMO Radar

3.1. Cognitive FDA MIMO Radar. To make the low probability of intercept, the parameters of target must be known to avoid the transmit signal leakage at the target location. So the FDA MIMO radar should adaptively sense the environment. This can be implemented through the feedback path from the receiver to the transmitter, which is a key characteristic of cognitive radar systems. A cognitive radar system

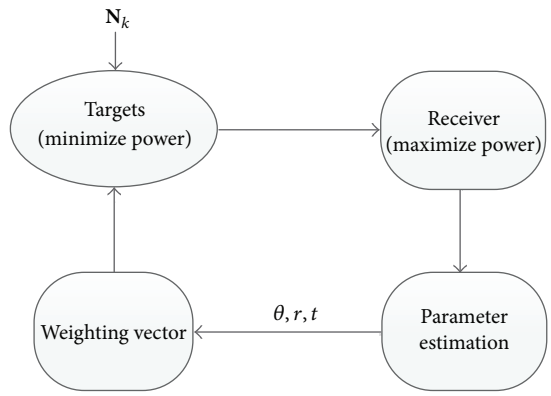

Figure 4: Block diagram of cognitive FDA feedback radar system.

constitutes a dynamic closed-loop feedback encompassing the transmitter, environment, and receiver. The radar adaptively estimated the target parameters through experience gained from interactions with the receiver and continually updates the receiver (Figure 4).

The proposed cognitive FDA LPI radar system is shown in Figure 3, including four subblocks. In the first part, the weighted design is carried out to minimize the energy at location of the target and maximize energy at the receiver. The designed transmit beam pattern propagates to the target. So the second part is the minimization of the energy of the target in the pulse duration by means of weighting transmit array and is polluted by the noise $\mathbf{N}_k$. The signals illuminated on the target are reflected and the reflected signals by target include the range and angle information. In the third part, the energy of the receiving area is maximized by the array weighting. The maximizing energy contribute to the signal detection at the receiver. Once the signals are detected by the receiver, the FDA MIMO radar signal is processed by matched filter, and the parameters are estimated by MUSIC algorithm in the last part. It can be seen that, utilizing the range dependent characteristic of the frequency diverse array, the detection probability of radar in the target can reach minimum, while, in the location of receive array, it can reach maximum. This means that the radar can have a good LPI performance.

3.2. Localization of FDA MIMO Radar. Consider an FDA MIMO radar equipped with M colocated transmitting elements and N colocated receiving elements. Assume the transmit and receive arrays are closely located, so that a target located in far-field can be seen by both of them at the same spatial angle. Each transmitting element sends out a distinct omnidirectional waveform $s_m(l)$, $m = 1, 2, 3, \ldots, M$ and $l = 1, 2, 3, \ldots, L$. Let $\mathbf{s}(l)$ be the vector collecting all these waveforms. The baseband equivalent model, in complex-valued form, of the transmitted signals from the mth transmit element can be expressed as [29–31]

$$a_m(\theta, r)\, s_m(l), \tag{10}$$

where

$$\begin{aligned} a_m(\theta, r) &= e^{j*2\pi((m-1)(d/\lambda)\sin\theta-(m-1)(\Delta f/c)r+(m-1)^2(\Delta f/c)d\sin\theta)} \\ &\approx e^{j*2\pi((m-1)((d/\lambda)\sin\theta-(\Delta f/c)r))} \end{aligned} \tag{11}$$

is the mth entry of the transmit steering vector with Δf being the frequency increment [26], where d is the element space, λ is the carrier wavelength, c denotes the light speed, and θ and r are the target angle and range, respectively.

After being reflected by the targets or interferences, the signals are received by the colocated receiving array. Taking the first element as a reference, the receive steering vector is

$$\mathbf{a}_r(\theta) = \left[1, e^{j\varphi}, e^{j2\varphi}, \ldots, e^{j(N-1)\varphi}\right]^T, \tag{12}$$

where $\varphi = 2\pi(d/\lambda)\sin\theta$ is the phase difference of the receive steering vector and $[\cdot]^T$ denotes the transpose operator. Therefore, the transmit steering vector at the receiving array is given by

$$\mathbf{a}_{\mathrm{tr}}(\theta, r) = \left[1, e^{j\phi_2}, e^{j2\phi_2}, \ldots, e^{j(M-1)\phi_2}\right]^T, \tag{13}$$

where $\phi_2 = 2\pi((d/\lambda)\sin\theta - (\Delta f/c)2r)$ is the phase difference of the transmit steering vector.

Suppose there are multiple targets located at (θ_i, r_i). The $N \times 1$ receive complex vector of the receiver observations can be written as

$$\mathbf{x}(l) = \sum_i \delta_i(\tau)\, \mathbf{a}_r(\theta_i)\, \mathbf{a}_{\mathrm{tr}}^T(\theta_i, r_i)\, \mathbf{s}(l) + \mathbf{n}(l), \quad l = 1, 2, \ldots, L, \tag{14}$$

where $\delta_i(\tau)$ represents the complex amplitude of the ith target source and $\mathbf{n}(l)$ is the $N \times 1$ additive zero-mean white Gaussian noise term with covariance matrix $\sigma^2\mathbf{I}$, with σ^2 being the noise power. Note that τ is the slow time and l is the fast time. Since $s_m(l)$ is orthogonal, the received signals

can be processed by a matched filter, which outputs an $M \times N$ matrix:

$$\begin{aligned}\mathbf{Y}(l) &= \left[\sum_{l=1}^{L}\mathbf{x}(l)\,\mathbf{s}^{H}(l)\right]\left[\sum_{l=1}^{L}\mathbf{s}(l)\,\mathbf{s}^{H}(l)\right]^{-1} \\ &= \sum_{i}\delta_i(\tau)\,\mathbf{a}_r(\theta_i)\,\mathbf{a}_{\mathrm{tr}}^{T}(\theta_i, r_i) + \mathbf{N},\end{aligned} \tag{15}$$

where

$$\mathbf{N} = \left[\sum_{l=1}^{L}\mathbf{n}(l)\,\mathbf{s}^{H}(l)\right]\left[\sum_{l=1}^{L}\mathbf{s}(l)\,\mathbf{s}^{H}(l)\right]^{-1}; \tag{16}$$

$[\cdot]^{-1}$ and $[\cdot]^{H}$ denote the matrix inverse operator and conjugate transpose operator, respectively, and $\sum$ denotes summation operator. Furthermore, it is easy to show that $\mathbf{N}$ is independent and identically distributed (i.i.d.) Gaussian entries with zero mean and variance σ^2. Stacking the columns of $\mathbf{Y}$, we obtain an $MN \times 1$ virtual data vector:

$$\mathbf{y} \triangleq \mathrm{vec}(\mathbf{Y}) = \sum_{i}\delta_i(\tau)\,\mathbf{a}(\theta_i, r_i) + \mathbf{n}, \tag{17}$$

where vec denotes vectorization operator and $\mathbf{n} \triangleq \mathrm{vec}(\mathbf{N})$ and

$$\mathbf{a}(\theta, r) \triangleq \mathbf{a}_{\mathrm{tr}}(\theta, r) \otimes \mathbf{a}_r(\theta) \tag{18}$$

denotes the joint transmit-receive virtual steering vector, in which $\otimes$ stands for the Kronecker product. The interference-plus-noise covariance matrix can be expressed as

$$\mathbf{R}_{\mathbf{y}} = \sum_{i}\alpha_i^2\,\mathbf{a}(\theta_i, r_i)\,\mathbf{a}^{H}(\theta_i, r_i) + \sigma^2\mathbf{I}, \tag{19}$$

where $\alpha_i^2 = E[\delta_i(\tau)\delta_i(\tau)^*]$ is the averaged power.

For independent target signals and noise, $\mathbf{R}_{\mathbf{y}}$ can be reformulated as

$$\begin{aligned}\mathbf{R}_{\mathbf{y}} &= \mathbf{A}_2(\theta, r)\begin{pmatrix}\mathbf{\Lambda} & 0\\ 0 & 0\end{pmatrix}\mathbf{A}_2(\theta, r)^{H} + \alpha_n^2\mathbf{I} \\ &= \begin{pmatrix}\mathbf{U}_A \vdots \mathbf{U}_n\end{pmatrix}\begin{pmatrix}\mathbf{\Lambda} + \sigma_S^2\mathbf{I} & 0\\ 0 & \sigma_{M-S}^2\mathbf{I}\end{pmatrix}\begin{pmatrix}\mathbf{U}_A \vdots \mathbf{U}_n\end{pmatrix}^{H},\end{aligned} \tag{20}$$

where $\mathbf{U}_A$ and $\mathbf{U}_n$ are the unitary matrices of signal and noise subspaces, respectively, $\mathbf{\Lambda}$ denotes the target signal power, and $\mathbf{I}$ is the unit matrix. The rank of $\mathbf{\Lambda} + \sigma_S^2\mathbf{I}$ is equal to the number of targets. Once the number of signals is obtained, the sizes of $\mathbf{U}_A$ and $\mathbf{U}_n$ are known accordingly. According to the MUSIC principle, the targets can be localized by searching the following peaks:

$$P(\theta, r) = \frac{1}{\mathbf{a}^{H}(\theta, r)\,\mathbf{U}_n\mathbf{U}_n^{H}\mathbf{a}(\theta, r)}. \tag{21}$$

3.3. LPI Beam Pattern Optimization Design. In this section, although we adopt the technology of MIMO radar, for radar signal detection, what we consider is whether beam pattern energy value formed by the transmit beam pattern in the air can be detected by the enemy reconnaissance aircraft or not and, at the receiver location, whether the signal energy can cause the response of receiver array sensor. Since the radar system of the enemy reconnaissance aircraft has not been determined, it is considered that the transmit signal is received by a single antenna and can also be matched with the filter.

In the above section, the target parameters are estimated by FDA MIMO radar, so according to the range and angle of the estimated parameters, we can design the transmit beam pattern of FDA MIMO radar. The problem of detecting a target in the presence of observes can be described as the following two assumptions. The first hypothesis is H_0; that is, received signal contains only noise $\mathbf{n}$. The other is H_1; that is, received signal is $\mathbf{x}(t)$. The detection problem can be formulated in terms of the following binary hypotheses test:

$$\begin{aligned}H_0 &: \mathbf{x} = \mathbf{n} \\ H_1 &: \mathbf{x} = \delta_0\left(\mathbf{w} \odot \mathbf{a}_{\mathrm{tr}}^{T}(\theta_0, r_0, t)\right)\mathbf{s}(t) + \mathbf{n}.\end{aligned} \tag{22}$$

Assuming that the noise vector is a zero-mean complex circular Gaussian vector with known positive definite covariance matrix:

$$E\left\{\mathbf{n}\mathbf{n}^{H}\right\} = \mathbf{M}. \tag{23}$$

According to the Neyman-Pearson criterion, if the phase of δ_0 is uniformly distributed, the generalized likelihood ratio test (GLRT) detector is given by

$$\left|\mathbf{x}^{H}\mathbf{M}^{-1}\left(\mathbf{w} \odot \mathbf{a}_{\mathrm{tr}}^{T}(\theta_0, r_0, t)\right)\right|^2 \underset{H_0}{\overset{H_1}{\gtrless}} G, \tag{24}$$

where G is the detection threshold set according to a desired value of the false alarm probability P_{fa}. An analytical expression of the detection probability P_d, for a given value of P_{fa}, is available for both cases of nonfluctuating and fluctuating target. In the former case (NFT) [32],

$$P_d = Q\left(\sqrt{2\left|\alpha\right|^2\left(\mathbf{w} \odot \mathbf{a}_{\mathrm{tr}} \odot \mathbf{s}\right)^{H}\mathbf{M}^{-1}\left(\mathbf{w} \odot \mathbf{a}_{\mathrm{tr}} \odot \mathbf{s}\right)}, \sqrt{-2\ln P_{\mathrm{fa}}}\right), \tag{25}$$

where Q denotes the Marcum Q function of order 1, while for the case of Rayleigh fluctuating target (RFT) with $E[|\alpha|^2] = \sigma_a^2$,

$$P_d = \exp\left(\frac{\ln P_{\mathrm{fa}}}{1 + \sigma_a^2\left(\mathbf{w} \odot \mathbf{a}_{\mathrm{tr}} \odot \mathbf{s}\right)^{H}\mathbf{M}^{-1}\left(\mathbf{w} \odot \mathbf{a}_{\mathrm{tr}} \odot \mathbf{s}\right)}\right). \tag{26}$$

Therefore, we can get the signal to noise ratio:

$$\text{SNR} = \begin{cases} |\alpha|^2 \left(\mathbf{w} \odot \mathbf{a}_{\text{tr}} \odot \mathbf{s}\right)^H \mathbf{M}^{-1} \left(\mathbf{w} \odot \mathbf{a}_{\text{tr}} \odot \mathbf{s}\right) & \text{NFT} \\ \sigma_a^2 \left(\mathbf{w} \odot \mathbf{a}_{\text{tr}} \odot \mathbf{s}\right)^H \mathbf{M}^{-1} \left(\mathbf{w} \odot \mathbf{a}_{\text{tr}} \odot \mathbf{s}\right) & \text{RFT}. \end{cases} \quad (27)$$

Our goal is to select the appropriate weighting vector $\mathbf{w}$ based on the above formula, so that the detection probability of radar at the target location can reach minimum, while at the location of receive array, it can reach maximum. We first observe that

$$\begin{aligned} &\left(\mathbf{w} \odot \mathbf{a}_{\text{tr}} \odot \mathbf{s}\right)^H \mathbf{M}^{-1} \left(\mathbf{w} \odot \mathbf{a}_{\text{tr}} \odot \mathbf{s}\right) \\ &\quad = \mathbf{w}^H \left(\mathbf{M}^{-1} \odot \left(\mathbf{a}_{\text{tr}} \mathbf{a}_{\text{tr}}^H\right)^* \odot \left(\mathbf{s}\mathbf{s}^H\right)^*\right) \mathbf{w} = \mathbf{w}^H \mathbf{R} \mathbf{w}, \end{aligned} \quad (28)$$

where $\mathbf{R} = \mathbf{M}^{-1} \odot (\mathbf{a}_{\text{tr}} \mathbf{a}_{\text{tr}}^H)^* \odot (\mathbf{s}\mathbf{s}^H)^*$. The covariance matrix of the target location is $\mathbf{R}_s = (\mathbf{M}^{-1} \odot (\mathbf{a}_{\text{tr}}(\theta_s, r_s, t) \mathbf{a}_{\text{tr}}^H(\theta_s, r_s, t))^* \odot (\mathbf{s}\mathbf{s}^H)^*)$ with θ_s, r_s denoting the location of target; the covariance matrix of FDA radar at the receiver location is $\mathbf{R}_r = (\mathbf{M}^{-1} \odot (\mathbf{a}_{\text{tr}}(\theta_r, r_r, t) \mathbf{a}_{\text{tr}}^H(\theta_r, r_r, t))^* \odot (\mathbf{s}\mathbf{s}^H)^*)$ with θ_r, r_r denoting the location of receiver. According to our goal problem, we know

$$\begin{aligned} \min_{\mathbf{w}} \quad & \mathbf{w}^H \mathbf{R}_s \mathbf{w} \quad \text{for } 0 \le t \le T \\ \text{s.t.} \quad & \|\mathbf{w}\|_2^2 = N, \\ \max_{\mathbf{w}} \quad & \mathbf{w}^H \mathbf{R}_r \mathbf{w} \quad \text{for } 0 \le t \le T \\ \text{s.t.} \quad & \|\mathbf{w}\|_2^2 = N. \end{aligned} \quad (29)$$

However, $\max_{\mathbf{w}} \mathbf{w}^H \mathbf{R}_r \mathbf{w}$ for $0 \le t \le T$ can be equivalent to

$$\min_{\mathbf{w}} \quad \frac{1}{\mathbf{w}^H \mathbf{R}_r \mathbf{w}} \quad \text{for } 0 \le t \le T. \quad (30)$$

Exploiting (29) and (30), the weighted optimization design problem can be formulated as a nonconvex optimization quadratic problem (QP):

$$\begin{aligned} \min_{\mathbf{w}} \quad & \frac{\mathbf{w}^H \mathbf{R}_s \mathbf{w}}{\mathbf{w}^H \mathbf{R}_r \mathbf{w}} \quad \text{for } 0 \le t \le T \\ \text{s.t.} \quad & \|\mathbf{w}\|_2^2 = N. \end{aligned} \quad (31)$$

In order to simplify the representation, the problem can be changed into

$$\begin{aligned} \min_{\mathbf{w}} \quad & \frac{\int_0^T \mathbf{w}^H \mathbf{R}_s \mathbf{w} \, dt}{\int_0^T \mathbf{w}^H \mathbf{R}_r \mathbf{w} \, dt} \\ \text{s.t.} \quad & \|\mathbf{w}\|_2^2 = N. \end{aligned} \quad (32)$$

For the weighted vector $\mathbf{w}$ is not related to time t, then there is

$$\int_0^T \mathbf{w}^H \mathbf{R} \mathbf{w} \, dt = \mathbf{w}^H \int_0^T \mathbf{R} \, dt \mathbf{w} = \mathbf{w}^H \mathbf{R}_T \mathbf{w}, \quad (33)$$

where

$$\begin{aligned} \mathbf{R}_T &= \int_0^T \mathbf{R} \, dt \\ &= \int_0^T \mathbf{M}^{-1} \odot \left(\mathbf{a}_{\text{tr}}(\theta, r, t) \mathbf{a}_{\text{tr}}^H(\theta, r, t)\right)^* \odot \left(\mathbf{s}\mathbf{s}^H\right)^* dt \\ &= \mathbf{M}^{-1} \odot \left(\mathbf{s}\mathbf{s}^H\right)^* \odot \int_0^T \left(\mathbf{a}_{\text{tr}}(\theta, r, t) \mathbf{a}_{\text{tr}}^H(\theta, r, t)\right)^* dt. \end{aligned} \quad (34)$$

Since $(\mathbf{a}_{\text{tr}}(\theta, r, t) \mathbf{a}_{\text{tr}}^H(\theta, r, t))^*$ is a relatively large matrix, in order to express its integral, we select the mn element as the representative, which is

$$\begin{aligned} &\int_0^T \left(\mathbf{a}_{\text{tr}}(\theta, r, t) \mathbf{a}_{\text{tr}}^H(\theta, r, t)\right)^* dt \\ &\quad = \int_0^T \left(e^{j2\pi((m-n)\Delta w t + (m-n)\Delta k r - k_0 (m-n) d \sin\theta)}\right)^* dt \\ &\quad = e^{j2\pi((m-n)\Delta k r - k_0 (m-n) d \sin\theta)} \frac{1 - e^{j2\pi((m-n)\Delta w T)}}{j2\pi (m-n) \Delta w}. \end{aligned} \quad (35)$$

Submitting (35) as the elements into (34), we can obtain $\mathbf{R}_T$. We express $\mathbf{R}_T$ at the target location as $\mathbf{R}_{sT}$ and at the receiver location as $\mathbf{R}_{rT}$. Equation (32) can be equivalent to

$$\begin{aligned} \min_{\mathbf{w}} \quad & \frac{\mathbf{w}^H \mathbf{R}_{sT} \mathbf{w}}{\mathbf{w}^H \mathbf{R}_{rT} \mathbf{w}} \\ \text{s.t.} \quad & \|\mathbf{w}\|_2^2 = N. \end{aligned} \quad (36)$$

Equation (36) is a nonconvex optimization quadratic problem (QP); it needs to be transformed into a convex problem. We define $\mathbf{W} = \mathbf{w}\mathbf{w}^H$. Equation (36) can be equivalent to the relaxation of

$$\begin{aligned} \min_{\mathbf{W}} \quad & \frac{\text{tr}\left(\mathbf{W}\mathbf{R}_{sT}\right)}{\text{tr}\left(\mathbf{W}\mathbf{R}_{rT}\right)} \\ \text{s.t.} \quad & \text{tr}\left(\mathbf{W}\right) = N \\ & \mathbf{W} \ge 0. \end{aligned} \quad (37)$$

This is an optimization problem of a linear fraction; in order to solve the problem, we add a parameter t and (37) can be equivalent to

$$\begin{aligned} \min_{\mathbf{W}} \quad & t \\ \text{s.t.} \quad & \frac{\text{tr}\left(\mathbf{W}\mathbf{R}_{sT}\right)}{\text{tr}\left(\mathbf{W}\mathbf{R}_{rT}\right)} \le t \\ & \text{tr}\left(\mathbf{W}\right) = N \\ & \mathbf{W} \ge 0 \end{aligned} \quad (38)$$

(1) Initialize $\mathbf{R}_{rT}$, $\mathbf{R}_{sT}$, with $t \in (0,1)$, let $t = t_0$, and $k = 0$
(2) Calculate the convex optimization problem (25) under the condition of fixing t_k
(3) Update t_k using dichotomy method, repeat the second step until the t^* is optimal;
(4) Solve $\mathbf{W}^*$ under t^*, calculate the rank $R = \text{rank}(\mathbf{W})$
(5) Loop iterations until $R = 1$;
(6) Decompose $\mathbf{W} = \mathbf{V}\mathbf{V}^H$;
(7) Find a nonzero solution of the system of linear equations
$$\mathbf{V}^H\mathbf{R}_o\mathbf{V} \cdot \mathbf{\Delta} = 0$$
where $\mathbf{\Delta}$ is an $R \times R$ matrix;
(8) The eigenvalue decomposition is carried on $\mathbf{\Delta}$, and the eigenvalues are $\delta_1, \delta_2, \ldots, \delta_R$;
(9) Determine k_0 and such that $|\delta_{k_0}| = \max\{|\delta_k| : 1 \le k \le R\}$;
(10) Calculate $\mathbf{W} = \mathbf{V}(\mathbf{I}_R - (1/\delta_{k_0})\mathbf{\Delta})\mathbf{V}^H$;
(11) Calculate $R = \text{rank}(\mathbf{W})$
(12) End loop

Algorithm 1: Rank-1 constrained solution procedure to solve the rank-one solution.

and the formula can also be equivalent to

$$\begin{aligned} \min_{\mathbf{W}} \quad & t \\ \text{s.t.} \quad & \text{tr}\left(\mathbf{W}\mathbf{R}_{sT}\right) \le t\left(\text{tr}\left(\mathbf{W}\mathbf{R}_{rT}\right)\right) \\ & \text{tr}\left(\mathbf{W}\right) = N \\ & \mathbf{W} \ge 0. \end{aligned} \tag{39}$$

The problem can be solved by combination using dichotomy and convex optimization. For a given time t, we can solve the following linear problem:

$$\begin{aligned} \text{find} \quad & \mathbf{W} \\ \text{s.t.} \quad & \text{tr}\left(\mathbf{W}\mathbf{R}_{sT}\right) \le t\left(\text{tr}\left(\mathbf{W}\mathbf{R}_{rT}\right)\right) \\ & \text{tr}\left(\mathbf{W}\right) = N \\ & \mathbf{W} \ge 0. \end{aligned} \tag{40}$$

We assume that the optimal solution t^* is obtained according to dichotomy. If $t < t^*$, then the feasible solution does not exist, and formula (40) has no solution. If $t^* < t$, the above formula can be solved, and $\mathbf{W}^*$ can be obtained. However, when we get the optimal solution $\mathbf{W}^*$ in $t \approx t^*$, we need to get the optimal $\mathbf{w}^*$ from $\mathbf{W}^*$. When $\mathbf{W}^*$ is a matrix of rank one, the eigenvector of the maximum eigenvalue $\mathbf{w}^*$ can be obtained by the eigendecomposition $\mathbf{W}^*$, while, in general, the solution optimized by the problem is not rank-one solution; sometimes the solution can be obtained by using the method of random approximation, but it is not sure whether the optimal results can be obtained.

In this paper, we use the rank constraint method to solve the rank-one solution for the problem. Since $\text{tr}(\mathbf{W}\mathbf{R}_{sT}) \le t(\text{tr}(\mathbf{W}\mathbf{R}_{rT}))$ can be changed as

$$\begin{aligned} &\text{tr}\left(\mathbf{W}\mathbf{R}_{sT}\right) - t\left(\text{tr}\left(\mathbf{W}\mathbf{R}_{rT}\right)\right) = \left(\mathbf{W}\mathbf{R}_{sT} - t\mathbf{W}\mathbf{R}_{rT}\right) \\ &\quad = \text{tr}\left(\mathbf{W}\left(\mathbf{R}_{sT} - t\mathbf{R}_{rT}\right)\right) = \text{tr}\left(\mathbf{W}\mathbf{R}_o\right), \end{aligned} \tag{41}$$

where $\mathbf{R}_o = \mathbf{R}_{sT} - t\mathbf{R}_{rT}$, (39) becomes

$$\begin{aligned} \min_{\mathbf{W}} \quad & t \\ \text{s.t.} \quad & \text{tr}\left(\mathbf{W}\mathbf{R}_o\right) \le 0 \\ & \text{tr}\left(\mathbf{W}\right) = N \\ & \mathbf{W} \ge 0. \end{aligned} \tag{42}$$

For fixed t, the dual problem of (42) is

$$\begin{aligned} \max_{y_1, y_2} \quad & Ny_1 \\ \text{s.t.} \quad & \mathbf{Z} = y_1\mathbf{I} - y_2\mathbf{R}_o \ge 0. \end{aligned} \tag{43}$$

Lemma 1. *Suppose that* $\mathbf{W}$ *is an* $N \times N$ *complex symmetric matrix of rank* R *and* $\mathbf{A}$ *is an* $N \times N$ *given Hermite symmetric matrix. Then, there is rank-one decomposition of* $\mathbf{W}$*:*

$$\begin{aligned} \mathbf{W} &= \sum_{j=1}^{r} \mathbf{w}_j \mathbf{w}_j^T, \\ \mathbf{w}_j^T \mathbf{A} \mathbf{w}_j &= \frac{\mathbf{A} \cdot \mathbf{W}}{R}, \end{aligned} \tag{44}$$

where $\mathbf{A} \cdot \mathbf{W} = \text{tr}\{\mathbf{A}\mathbf{W}\}$.

According to Lemma 1, the solution can be obtained by using the algorithm described in Algorithm 1 [33].

4. Simulation Results

We assume that the array parameters of FDA are as follows: the array element number is $M = N = 8$, the reference carrier frequency of the first array element is $f_0 = 10\,\text{GHz}$, the spacing between elements is $d = \lambda/2$, light speed is $c = 3 \times 10^8$ m/s, frequency offset between array elements is $\Delta f = 10\,\text{KHz}$, and pulse duration is $T = 1/\Delta f$. The additive noise is modeled as complex Gaussian zero-mean spatially and temporally white random sequences that has identical variance in the array sensors.

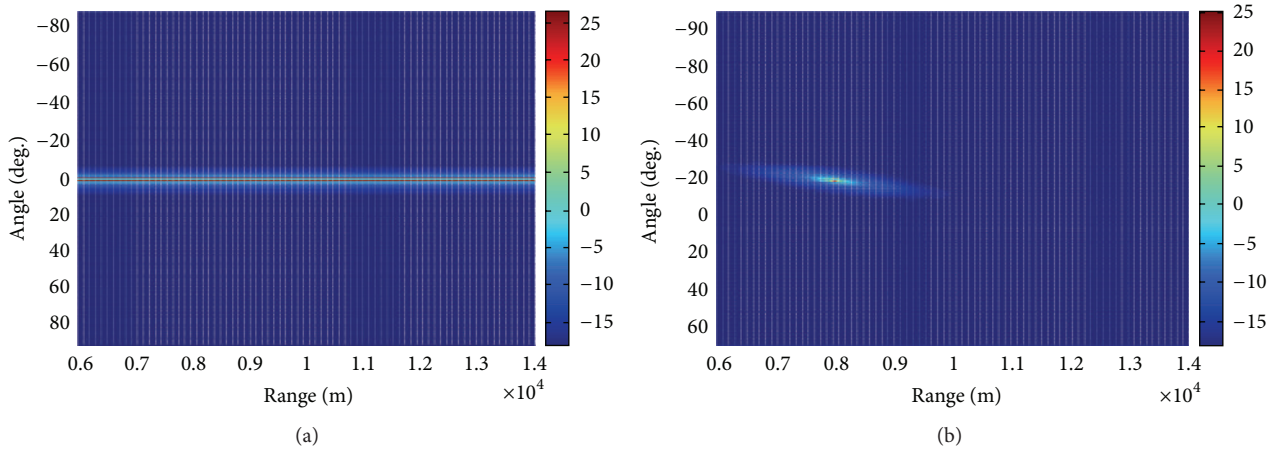

Figure 5: Comparison of estimated parameters of power spectrum. (a) Conventional MIMO radar; (b) FDA MIMO radar.

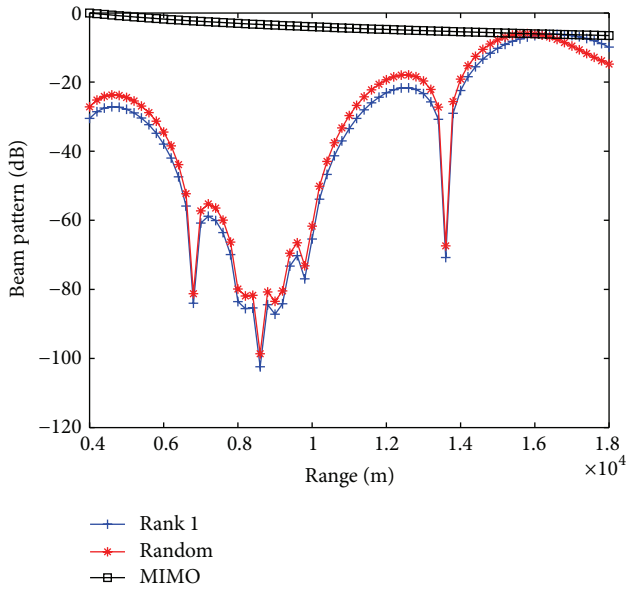

Figure 6: Comparison of the energy distribution of the beam pattern.

Example 1 (localization of FDA MIMO radar). Comparison of estimated parameters between conventional MIMO radar and FDA MIMO radar: location of target reconnaissance aircraft is (0°, 8 km). Figure 5 shows the parameter estimation of the conventional phased-array MIMO radar and the FDA MIMO radar. Figure 5(a) shows that the parameter estimation of the conventional phased-array MIMO radar is a straight line. It means that the target angle can only be estimated by the conventional MIMO radar. Figure 5(b) shows that the MUSIC power spectrum of the FDA MIMO radar is a point. It means that FDA MIMO radar can estimate both the angle and range of the target, which can locate the target directly. Therefore, the FDA MIMO radar is better at range estimation than the traditional MIMO radar.

Example 2 (LPI performance analysis). Comparison results of the energy distribution of beam pattern in the range dimension between conventional MIMO radar (MIMO in the figures), FDA MIMO radar based on rank-one constrain, and FDA MIMO radar based on random approximation are shown in Figure 6.

As shown in Figure 6, we can get the following: (1) according to the energy distribution of the beam pattern of conventional MIMO radar, it can be seen that the energy distribution of the conventional MIMO radar decreases with the increase of the propagation range. However, the energy in the target location cannot be obviously reduced, which cannot achieve the expected low probability of interception performance. And because of the high overall energy of the conventional MIMO radar, it is very easy to be detected by the enemy reconnaissance aircraft. (2) According to the radar equation, the energy of the beam pattern of the FDA radar will decrease with the increase of the range. But, as shown in

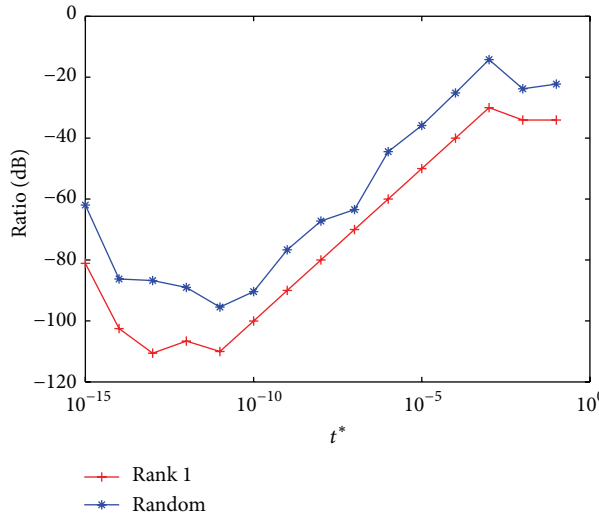

Figure 7: Selection of target and receiver power ratio factors.

Figure 6, the energy of the radar signal at the target location, after weighting optimization by our proposed algorithm, is only about −80 dB, which is far lower than that of the conventional MIMO radar. And, after the target's reflection, the receiver's energy reaches the maximum, as shown in Figure 6, and the location of the receiver, which is just the position of 16 km, corresponds to the maximum energy point. The reason is that the phase of the FDA radar signal changes with the range; that is, at the radar receiver, the reflected signal angle is not changed, but the distance is changed, so the signals phases at receiver are different from that of the target, and then the energy at the receiver reaches the maximum value with the optimization of the weighted algorithm. This also is the unique advantage of the FDA MIMO radar in the low probability of intercept. (3) Figure 6 also gives beam pattern energy distribution based on the minimization of the random approximation. The results showed that it does not outperform the rank-one optimization method. Its energy distribution at the target is larger, which is more likely to be detected by reconnaissance aircraft. At the receiver, the time durability of its energy distribution is not good.

Figure 7 shows the relationship between power ratio factor t of the target and receiver energy distribution (used in the dichotomy) and the energy ratio of the two positions. From Figure 7, in a certain range, the energy ratio of the two positions is linear with t. But the linear relationship is broken when t is very small for the reason of optimization; the energy ratio of the two positions no longer decreases with the decrease of t; it may increase. This provides the basis for the selection of t. We do not have to choose a very small t, but we need to select t corresponding to the minimum energy ratio. Therefore, in the experiment of this paper, $t^* = 10^{-11}$ is chosen.

Comparison results of the target detection probability at the target and at the receiver of FDA MIMO radar and the MIMO radar are given in Figure 8, where MIMO represents conventional MIMO radar. For the transmitted signal of the conventional MIMO radar, the probability of being detected at the target is higher than that at the receiver.

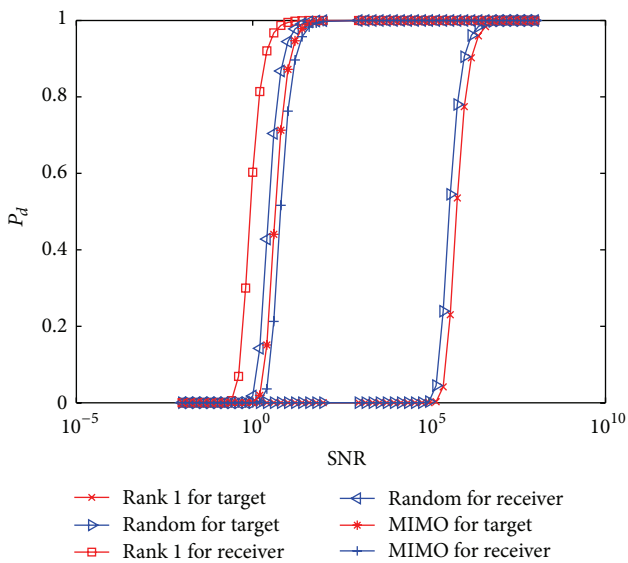

Figure 8: Comparison of detection probability.

This is because the signal received by the receiver is a signal of the target's reflection; it has two times time delay compared to that of the signal at the target. Thus, the signal energy is attenuated to half. This causes the lower detection probability at the receiver and higher detection probability at the target. However, this problem has been avoided completely by FDA MIMO radar. We can see from Figure 8 that, at the target, the energy of the beam pattern is very small, so the low detection probability of the target is realized. While, at the receiver, its energy is relatively larger, the high detection probability is realized.

5. Conclusion

This paper proposes a cognitive FDA MIMO radar with low probability of intercept design. Inspired by cognitive radar scheme, two steps are proposed to achieve the LPI.

The first step is to estimate the target parameters by FDA MIMO radar; the second step is to design the transmit array to minimize the energy in which the target is located and maximize the energy of the receiver. In the second step, the convex optimization and dichotomy are jointly used to obtain the optimal weighting matrix. The rank constraints method is used to derive the weighting vector. Simulation results show that the rank constraints method is better than the rand minimization in detection performance. Moreover, it decreases the interception risk and improve the receive probability. Therefore, compared with conventional radar, the designed FDA-MIMO radar has better LPI performance.

Competing Interests

The authors declare that they have no competing interests.

Acknowledgments

This work was supported in part by the Program for New Century Excellent Talents in University under Grant no. NCET-12-0095, the National Natural Science Foundation of China under Grant no. 61563032, and the University Research Project of Department of Education of Gansu province under Grant no. 2015A-043.

References

[1] D. C. Schleher, *Introduction to Electronic Warfare*, Artech House, Boston, Mass, USA, 1986.

[2] A. G. Stove, A. L. Hume, and C. J. Baker, "Low probability of intercept radar strategies," *IEEE Proceedings—Radar Sonar and Navigation*, vol. 151, no. 5, pp. 249–260, 2004.

[3] G. Schrick and R. G. Wiley, "Interception of LPI radar signals," in *Proceedings of the IEEE International Radar Conference*, pp. 108–111, Arlington, Va, USA, May 1990.

[4] G. T. Oreilly, T. C. Pierce, and R. R. McElroy, "Track-while-scan quiet radar," in *Proceedings of the 15th Annual Electronics and Aerospace Systems Conference*, pp. 369–374, Washington, DC, USA, September 1982.

[5] D. E. Lawrence, "Low probability of intercept antenna array beamforming," *IEEE Transactions on Antennas and Propagation*, vol. 58, no. 9, pp. 2858–2865, 2010.

[6] A. Basit, I. M. Qureshi, W. Khan, I. Ulhaq, and S. U. Khan, "Hybridization of cognitive radar and phased array radar having low probability of intercept transmit beamforming," *International Journal of Antennas and Propagation*, vol. 2014, Article ID 129172, 11 pages, 2014.

[7] P. Antonik, M. C. Wicks, H. D. Griffiths, and C. J. Baker, "Frequency diverse array radars," in *Proceedings of the IEEE Radar Conference*, pp. 215–217, IEEE, Verona, NY, USA, April 2006.

[8] M. C. Wicks and P. Antonik, "Frequency diverse array with independent modulation of frequency, amplitude, and phase," US Patent 7,319,427, 2008.

[9] P. Antonik and M. C. Wicks, "Method and apparatus for simultaneous synthetic aperture and moving target indication," US Patent, Application 20080129584, 2008.

[10] P. Antonik, M. C. Wicks, H. D. Griffiths, and C. J. Baker, "Multi-mission multi-mode waveform diversity," in *Proceedings of the IEEE Radar Conference*, pp. 580–582, Verona, NY, USA, April 2006.

[11] P. Antonik and M. C. Wicks, "Method and apparatus for a frequency diverse array," U.S.A Patent 7.511,665B2, March 2009.

[12] P. Antonik, *An investigation of a frequency diverse array [Ph.D. thesis]*, University College London, London, UK, 2009.

[13] A. Aytun, *Frequency diverse array radar [M.S. thesis]*, Naval Postgraduate School, 2010.

[14] S. Brady, *Frequency diverse array radar: signal characterization and measurement accuracy [M.S. thesis]*, Air Force Institute of Technology, Wright-Patterson Air Force Base, Ohio, USA, 2010.

[15] M. Secmen, S. Demir, A. Hizal, and T. Eker, "Frequency diverse array antenna with periodic time modulated pattern in range and angle," in *Proceedings of the IEEE Radar Conference*, pp. 427–430, Boston, Mass, USA, April 2007.

[16] P. Baizert, T. B. Hale, M. A. Temple, and M. C. Wicks, "Forward-looking radar GMTI benefits using a linear frequency diverse array," *Electronics Letters*, vol. 42, no. 22, pp. 1311–1312, 2006.

[17] P. F. Sammartino and C. J. Baker, "The frequency diverse bistatic system," in *Proceedings of the 4th Waveform Diversity and Design Conference*, pp. 155–159, Orlando, Fla, USA, February 2009.

[18] J. Farooq, M. A. Temple, and M. A. Saville, "Application of frequency diverse arrays to synthetic aperture radar imaging," in *Proceedings of the International Conference on Electromagnetics in Advanced Applications (ICEAA '07)*, pp. 447–449, Torino, Italy, September 2007.

[19] J. Farooq, M. A. Temple, and M. A. Saville, "Exploiting frequency diverse array processing to improve SAR image resolution," in *Proceedings of the IEEE Radar Conference*, pp. 1–5, IEEE, Rome, Italy, May 2008.

[20] J. Farooq, *Frequency diversity for improving synthetic aperture radar imaging [Ph.D. thesis]*, Air Force Institute of Technology, Wright-Patterson, Ohio, USA, 2009.

[21] Y. Wang, W.-Q. Wang, and H. Shao, "Frequency diverse array radar Cramér-Rao lower bounds for estimating direction, range, and velocity," *International Journal of Antennas and Propagation*, vol. 2014, Article ID 830869, 15 pages, 2014.

[22] V. Ravenni, "Performance evaluations of frequency diversity radar system," in *Proceedings f the European Radar Conference (EuRAD '07)*, pp. 436–439, IEEE, Munich, Germany, October 2007.

[23] W.-Q. Wang, "Range-angle dependent transmit beampattern synthesis for linear frequency diverse arrays," *IEEE Transactions on Antennas and Propagation*, vol. 61, no. 8, pp. 4073–4081, 2013.

[24] P. F. Sammartino, C. J. Baker, and H. D. Griffiths, "Frequency diverse MIMO techniques for radar," *IEEE Transactions on Aerospace and Electronic Systems*, vol. 49, no. 1, pp. 201–222, 2013.

[25] L. Zhuang and X. Liu, "Application of frequency diversity to suppress grating lobes in coherent MIMO radar with separated subapertures," *Eurasip Journal on Advances in Signal Processing*, vol. 2009, Article ID 481792, 2009.

[26] W.-Q. Wang, "Phased-MIMO radar with frequency diversity for range-dependent beamforming," *IEEE Sensors Journal*, vol. 13, no. 4, pp. 1320–1328, 2013.

[27] W.-Q. Wang and H. Shao, "Range-angle localization of targets by a double-pulse frequency diverse array radar," *IEEE Journal on Selected Topics in Signal Processing*, vol. 8, no. 1, pp. 106–114, 2013.

[28] W.-Q. Wang and H. C. So, "Transmit subaperturing for range and angle estimation in frequency diverse array radar," *IEEE*

Transactions on Signal Processing, vol. 62, no. 8, pp. 2000–2011, 2014.

[29] K. Gao, H. Chen, H. Shao, J. Cai, and W.-Q. Wang, "Impacts of frequency increment errors on frequency diverse array beampattern," *EURASIP Journal on Advances in Signal Processing*, vol. 2015, article 34, 2015.

[30] K. Gao, H. Shao, J. Cai, H. Chen, and W.-Q. Wang, "Frequency diverse array MIMO radar adaptive beamforming with range-dependent interference suppression in target localization," *International Journal of Antennas and Propagation*, vol. 2015, Article ID 358582, 10 pages, 2015.

[31] K. Gao, H. Chen, J. Cai et al., "Impact of frequency increment errors on frequency diverse array mimo adaptive beamforming and target localization," *Digital Signal Processing*, vol. 44, pp. 58–67, 2015.

[32] A. D. Maio, S. D. Nicola, Y. Huang, S. Zhang, and A. Farina, "Code design to optimize radar detection performance under accuracy and similarity constraints," *IEEE Transactions on Signal Processing*, vol. 56, no. 11, pp. 5618–5629, 2008.

[33] Y. Huang and D. P. Palomar, "Rank-constrained separable semidefinite programming with applications to optimal beamforming," *IEEE Transactions on Signal Processing*, vol. 58, no. 2, pp. 664–678, 2010.